THE AMERICAN SOCIETY OF MECHANICAL ENGINEERS
345 E. 47th St., New York, N.Y. 10017

96-GT-157

Unsteady flow in the vaned diffuser of a medium specific speed pump

Felix A. Muggli, Donald Wiss, Klaus Eisele, Zhengji Zhang, Michael V. Casey
Fluid Dynamics Laboratory
Sulzer Innotec
Winterthur
Switzerland

Paul Galpin
Advanced Scientific Computing
Waterloo, Ontario
Canada

ABSTRACT

This paper describes experimental and computational work to examine the unsteady flowfield in the vaned diffuser of a medium specific speed pump. The time periodic flowfield in the diffuser has been examined experimentally with laser optical techniques and with unsteady pressure transducers. The flow has been computed with a general purpose Navier-Stokes CFD code, whereby the unsteady effects have been simulated by a time periodic inlet profile which translates across the diffuser inlet and represents the wakes and potential interaction from the impeller. Comparisons of a steady simulation with time-average inlet conditions, an unsteady simulation with a time periodic inlet profile and the time-average of the unsteady simulation are used to validate the code developments and to examine features of the unsteady flow through the diffuser. Comparisons with experimental data identify that this simple computational model with a time periodic inlet profile is able to simulate the convection and decay of disturbances passing through the diffuser.

NOMENCLATURE

B_2	impeller exit width
B_3	diffuser vane inlet width
D_0	impeller hub diameter
D_1	impeller shroud diameter
D_2	impeller exit diameter
D_3	diffuser vane inlet diameter
D_4	diffuser vane exit diameter
D_5	diameter of return channel
n	impeller speed
P	static pressure
P_{total}	total pressure
U	velocity in x direction
u_2	circumferential velocity of impeller exit
V	velocity in y direction
W	$=\sqrt{U^2+V^2}$, velocity magnitude
x, y, z	coordinates
ΔP	pressure difference
ΔP^*	dimensionless static pressure pulsation
Θ	opening angle
ρ	density

INTRODUCTION

It is well known that the close proximity of the impeller and diffuser of a centrifugal turbomachine causes a strong interaction between the flow in both components. This interaction has a large influence on the stability of the operating characteristic and on the pressure pulsations, vibrations and noise generated in both radial compressors and radial pumps. This paper describes ongoing experimental and computational work aimed at examining the nature of this interaction for radial turbomachinery.

The practical relevance of the unsteady flowfield at the impeller outlet on pump design can be found in the recent EPRI design guidelines (Gülich et al. 1992, Gülich and Bolleter 1992). The wakes from the impeller blades cause exciting forces and noise at the blade passing frequency and at its higher harmonics. Recent work of Chu et al. (1995) investigated the relationship between unsteady flow and noise in centrifugal pumps. In poor designs excessive loads due to these forces can cause failure of the diffuser vanes and damage to the impeller shroud (side plate), especially if these pulsations occur at a resonant natural frequency. Similar problems can also occur in compressors, especially in high pressure process compressors or in compressors with shroudless impellers. The EPRI design guideline for pumps (Gülich et al. 1992) specifies that a wider spacing between the diffuser inlet vanes and the impeller outlet needs to be selected at higher impeller tip speeds to avoid these noise and vibration problems. This is a compromise which militates against the requirements for optimum

Presented at the International Gas Turbine and Aeroengine Congress & Exhibition
Birmingham, UK — June 10-13, 1996

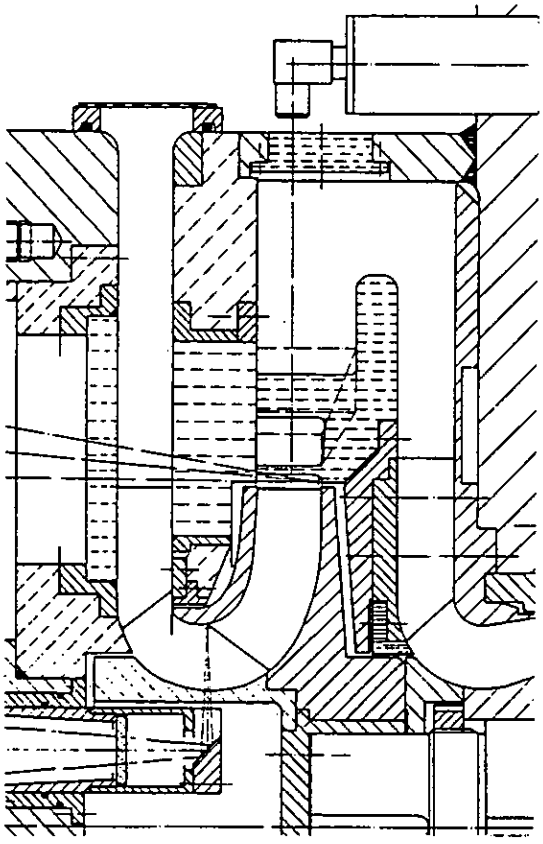

Fig. 1 Test pump with vaned diffuser

aerodynamic design, which would prefer the diffuser channels to be longer in order to achieve higher diffusion levels.

This paper describes both experimental and computational work aimed at examination of the unsteady flowfield in a medium specific speed pump diffuser with a relatively small radial gap between the impeller and the diffuser (4% of the impeller diameter). The detail of the unsteady flowfield in the pump diffuser has been examined experimentally with laser optical techniques (Laser Doppler Anemometry, LDA and Particle Tracking Velocimetry, PTV) and with unsteady pressure transducers in a specially designed test pump with good optical access. These measurements are being used to provide a systematic database of experimental data for evaluation of CFD methods for examining the flow in diffusers, see Casey et al. (1995a, 1995b). The objective of the current work is to describe progress in the use of these measurements for the validation of a general purpose commercial CFD code "TASCflow" (ASC 1994) for the computation of unsteady flow in turbomachinery applications.

It is currently impractical in industry to examine in full detail the unsteady diffuser-impeller interaction using three-dimensional Navier-Stokes simulations of an entire pump. A simulation of the three-dimensional unsteady interaction between the impeller and diffuser blade rows of a pump would take orders of magnitude more CPU time than is currently available for a routine simulation of a single blade row on a typical high power workstation used in industry. Despite the complexity of such calculations, some first university-based attempts at the numerical simulation of this type of unsteady interaction have already appeared in the technical literature, for example the three-dimensional viscous calculations in a radial compressor presented by Dawes (1994) and the two-dimensional turbine calculations presented by Giles and Haimes (1993). At the present state of the art of CFD in an industrial design environment, however, simpler calculation methods are needed to examine this unsteady flow.

In this paper the simplest possible form of unsteady calculation for examination of the unsteady flowfield in the diffuser is used, whereby the unsteady flow coming from the impeller has been modelled by a time periodic inlet profile which rotates around the diffuser inlet with the rotational speed of the impeller. This neglects any reverse interaction of the diffuser on the impeller flowfield. Additional simplifications included in these simulations are that a representative two-dimensional section of the diffuser has been simulated and a pitch change in the impeller flow has been assumed so that a representative section with two blade passages of the diffuser can be calculated.

Despite these simplifications, the simulation is still extremely difficult, as it includes both the strong potential interactions and the wake/blade interactions occurring in the diffuser due to the passage of the impeller across the inlet boundary of the diffuser computational domain. In order to get a clearer understanding of some of these effects three different types of comparison are presented in the paper. First, a steady flow solution with a constant mean inlet condition is compared to the time-average of the unsteady solution as a means of assessing the importance of the unsteady effects on the flowfield. Second, the unsteady solution at various time intervals is compared to the time-average of the unsteady solution to identify important features of the unsteady flowfield. Finally, the results of the unsteady calculations are compared with the detailed time-periodic flow measurements in the vaned diffuser of the test pump. These comparisons are used to identify to what extent this simple model of a time periodic profile is able to simulate the measured details of the unsteady flow and to validate the code developments for this type of unsteady turbomachinery simulation.

TEST RIG AND TEST GEOMETRY

A dedicated closed loop test rig for optical measurements in a single stage medium specific speed pump has been designed, as shown in Fig. 1. The geometry of the pump used for these tests represents a middle stage of a medium specific speed multistage pump. The pump inlet geometry in the rig was designed to provide a clean uniform flow at pump inlet. The diffuser geometry in the rig has been modified slightly compared to the standard geometry for normal applications to provide good optical access and to improve the specification of the boundary conditions for numerical simulations. In particular, the return channel was lengthened compared with a normal middle stage diffuser so that a clearly defined outlet boundary condition was available for the diffuser simulations. Further details of the design of test rig can be found in Eisele et al. (1992). Earlier work on the same test rig included detailed measurements and steady numerical computations of the flow in the pump impeller, Schachenmann et al. (1993), Eisele et al. (1993), and diffuser, Casey et al. (1995a, b).

TABLE 1: Main dimensions of the pump

Impeller	Diffuser
D_0 = 140 mm	D_3 = 364 mm
D_1 = 208 mm	D_4 = 496 mm
D_2 = 350 mm	D_5 = 570 mm
B_2 = 32.9 mm	B_3 = 34.5 mm
n = 1000 rpm	
Vanes: 7	Vanes: 12

The main dimensions of the impeller and the diffuser are listed in table 1. It is of interest to note that relative to the impeller outlet radius, the diffuser vane inlet radius is very close to the impeller, at D_3/D_2=1.04 giving a very short (4%) vaneless radial gap between the impeller and the diffuser. The diffuser vanes are also relatively short with a vane outlet radius at D_4/D_3=1.36. The diffuser is not of constant axial width and within the diffuser channels the diffuser area increases both between the vanes and between the endwalls by the use of a sloping endwall on the hub side of the diffuser, see figure 1. The sloping endwall gives rise to a non-axisymmetric hub wall and also leads to a very highly loaded diffuser design with a channel length to inlet width ratio of 4.8, an equivalent 2D diffuser opening angle of 2θ=14°, and an area ratio of 2.55. In the typical diffuser design charts of Reneau et al. (1967) the diffuser is just below the transition from attached flow to transitory stall.

Two diffusers of similar geometry were used in this work. For the flow visualization and PTV measurements a perspex model was used and for the LDA measurements an aluminium diffuser of similar geometry was manufactured. The perspex model was also equipped with pressure transducers for static and dynamic measurements of the wall pressures.

MEASURING METHODS

The unsteady flow in the diffuser was investigated in the test pump by the use of Laser Doppler Anemometry, Laser Particle Tracking Velocimetry, flow visualization and dynamic pressure measurements. The results of some of these experiments and details of the experimental methods used are reported in earlier papers by Eisele et al. 1994 and Casey et al. 1995a. The 3-D flowfield in the diffuser was measured at 5 different flow rates from the best efficiency point to deep partload. The LDA and PTV measurement data was triggered by the impeller rotation so that time periodic data at the impeller outlet was obtained. Two dimensional flowfield data obtained from the investigations at the best efficiency point of the impeller have been used to compare with the unsteady simulations described in this paper.

Particular attention was given in the design of the test rig to the provision of optical windows to enable LDA (Laser Doppler Anemometry) and PTV (Particle Tracking Velocimetry) measurements to be made, both in the impeller and in the diffuser. The test loop was also made of stainless materials and filled with demineralised water to ensure clean optical access. For the optical measurements seeding of the water was necessary and glass particles of 4μm were used for LDA measurements and polystyrene particles of 60μm for PTV measurements.

Laser Doppler Anemometry (LDA)

A two colour Dantec fiber LDA with a PDA processor was used for the measurements in the pump diffuser. For further details of the measurement techniques, see Eisele et al. (1994), Casey et al. (1995a) and Zhang et al. (1995). The main interest of the LDA measurements was to examine the unsteady flow in the semi-vaneless region of the diffuser, so most of the LDA measurement points were localized in this region. The three-dimensional velocity field was measured but the measurement data presented here includes only the radial and circumferential components of the measured velocities. The LDA apparatus was triggered by the rotational position of the impeller so that the unsteady flowfield relative to the impeller vane position could be examined.

Laser Particle Tracking Velocimetry (PTV)

A Laser particle tracking velocimetry technique (Eisele et al., 1995) was applied to obtain two-dimensional steady and unsteady flow field information in the diffuser. The illumination source was a continuous wave argon ion laser with a glass fiber light sheet probe. This fiber probe was mounted in the pump (Fig. 1). The measurement zone was illuminated through a window and a perspex diffuser vane. Multiple exposures were realized through a CCD camera with a high speed shutter and with an integrated light amplifier. The shutter of this camera is computer controlled and both the shutter of the camera and the frame grabber were synchronized with the rotational position of the pump impeller. The direction of the velocity vector was determined by tagged particle traces with long and short exposures using a particle tracking software following the procedures outlined by Grant (1990).

Dynamic pressure measurements

In the test pump pressure transducers are located on both endwalls of the diffuser. The location of the transducers are marked in Fig. 11. For the measurement of the dynamic pressure very small transducers are used. These transducers were developed for measurements of the human blood pressure in vivo. The main geometric and electrical data of these piezo-resistive transducers are listed in table 2:

TABLE 2: Characteristics of the pressure transducers

Diameter:	2.7 mm
Max. Overload Pressure	20 bar
3 db Cut off Frequency	100 kHz
Sensitivity	4 mV/bar
Linearity Factor	0.4 %

The signals of these transducers were amplified and filtered and as a data acquisition system a PC with a digital/analog converter was used. It was also possible to capture these pressure signals synchronized with the LDA measurements by using the LDA data acquisition system (Eisele et al. 1992). The unsteady static pressure measurements on the endwalls at the impeller outlet were combined with data from the LDA measurements to provide a unsteady inlet total pressure for the simulations.

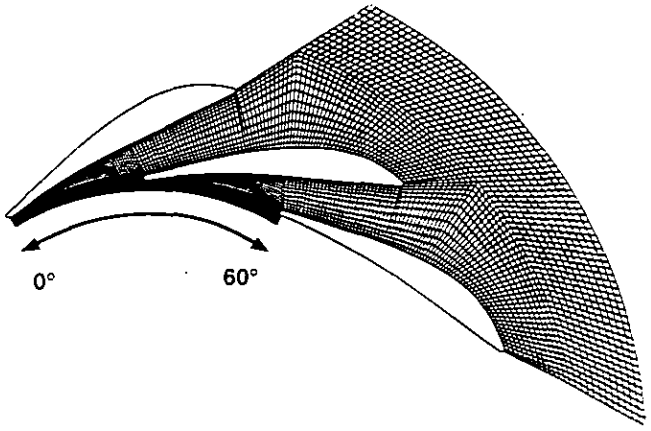

Fig. 2 Computational grid

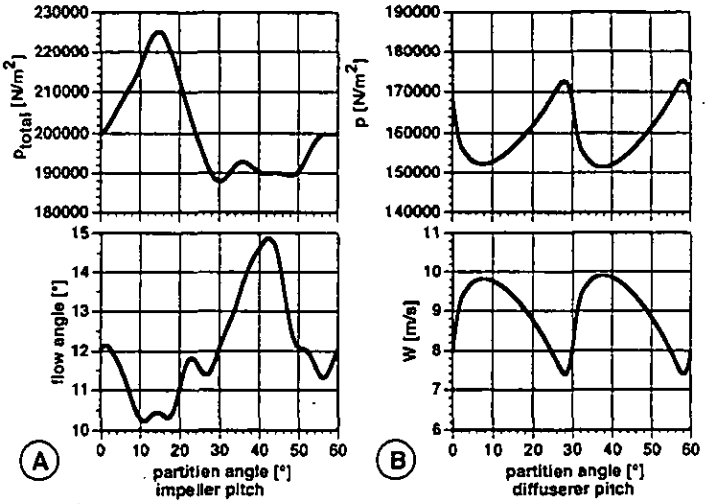

Fig. 3 Inlet boundary conditions for the simulation: A) Time periodic total pressure profile and flow angle B) Resulting time-averaged static pressure and velocity profile

NAVIER STOKES CODE WITH k-ε TURBULENCE MODEL

A commercial software package was used for this study, the code "TASCflow" from ASC (1994). The Reynolds-averaged Navier-Stokes equations are solved by this code in strong conservation form. The transport equations are discretized using a conservative finite-volume method. Both incompressible and compressible flows can be analyzed. Turbulence effects are modelled using the k-ε turbulence model. Details regarding the theoretical basis and handling of the boundary conditions of the code are reported in full by ASC (1994). Many successful reports of the application of this code to turbomachinery problems have been reported in the technical literature, for example, it has been used for pump impellers by Schachenmann et al. (1993), for steady flow in this vaned pump diffuser by Casey et al. (1995b) and for a transonic compressor rotor by Dalbert and Wiss (1995).

SIMULATIONS OF A TWO-DIMENSIONAL PUMP DIFFUSER

The computations presented here represent the first step in a series of calculations that are planned to examine the unsteady flowfield and the impeller and diffuser interactions. In this paper the simplest possible form of unsteady calculation for the unsteady flowfield in the diffuser is used, whereby the unsteady flow coming from the impeller has been modelled by a time periodic inlet profile which rotates around the diffuser inlet with the rotational speed of the impeller. This neglects any reverse interaction of the diffuser on the impeller flowfield. The inlet boundary conditions used for this diffuser simulation are taken from the measurements at the pump outlet. Subsequent computations will make use of inlet boundary conditions taken from an impeller simulation and ultimately it is intended to carry out a full unsteady impeller diffuser simulation.

Simplifications and assumptions

To reduce the amount of computer memory, disk storage space and the computation time for this initial validation phase of the project, it was decided to carry out two-dimensional simulations. Furthermore, only two blade to blade passages of the diffuser, which has 12 vanes, were discretized by the computational grid. To avoid non-periodic boundary conditions at the borders of the computational domain, the impeller was modelled with six blades instead of seven on the real wheel. This means that one impeller flow channel is always matched to two diffuser flow channels but requires an artificial pitch change in the measurement data of the impeller.

Geometry and grid

The vaned diffuser of the radial pump test rig (Fig. 1) was modelled at mid span by a two-dimensional computational grid (Fig. 2). The grid starts at the trailing edge of the impeller blades and extends radially to the endwall of the pump casing. It covers two blade to blade sections of the diffuser. It consists of seven grid blocks, five H-grids and 2 pinched H-grids including a total of 6350 nodes in the 2D-plane. It can easily be expanded in axial direction for future three-dimensional simulations.

At the locations where pressure transducers are in the test rig, a node was placed in the computational grid. Therefore it is possible to compare the calculated and measured pressures directly without the need of any interpolation.

Boundary conditions

The pump diffuser simulations were carried out with water as the fluid, and therefore incompressible flow with constant density could be assumed. All the surfaces of the diffuser vanes were defined as solid walls. Two diffuser channels were modelled and the adjacent regions of the full diffuser were modelled by the appropriate use of periodic boundary conditions.

At the inlet of the computational domain, a time periodic profile was used to simulate the rotating flow pattern coming from the impeller. This time periodic profile covers one blade to blade pitchwise section of the impeller. As mentioned above, the effective number of impeller blades for this simulation was reduced from seven to six to

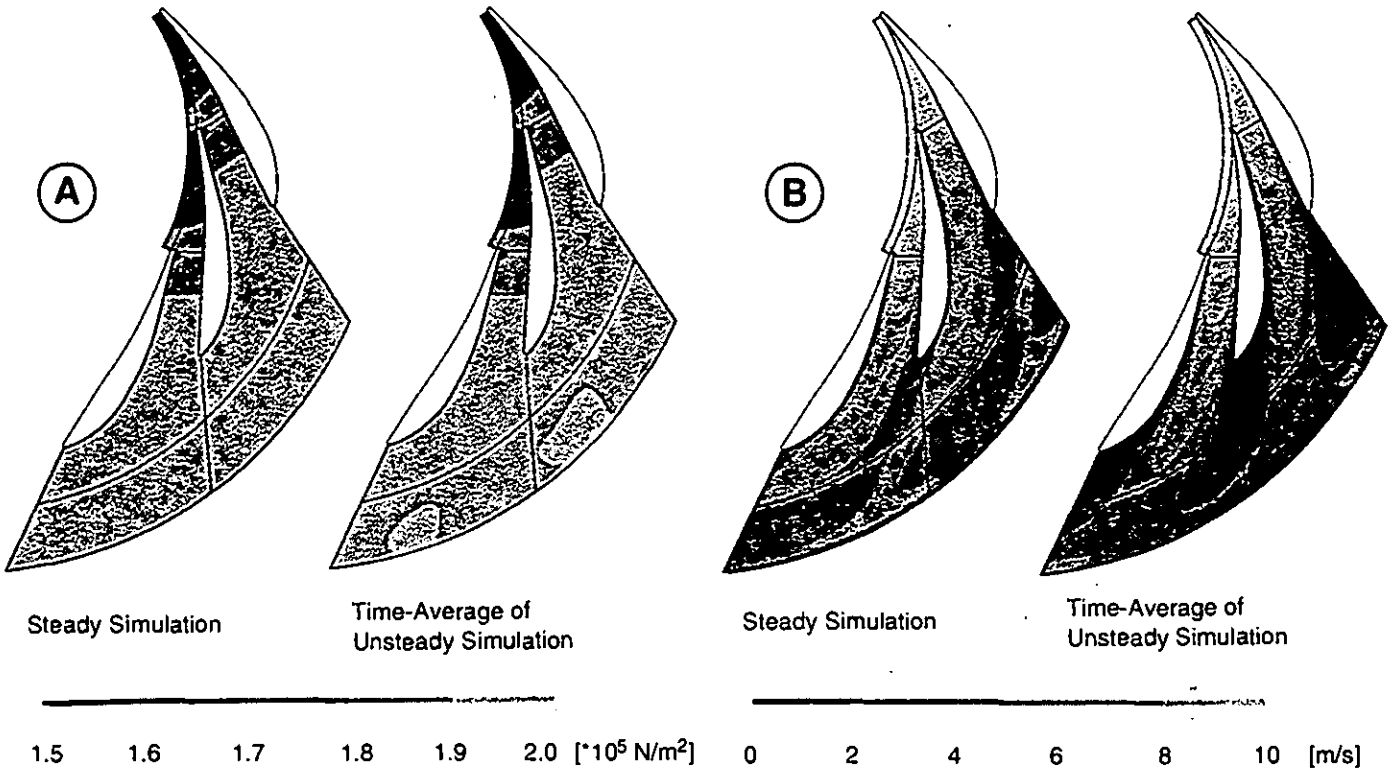

Fig. 4 Comparison of steady simulation and time-average of unsteady simulation:
A) Static pressure p
B) Velocity magnitude w

obtain an integer number for the vane to blade pitch ratio (twice as many diffuser vanes as impeller blades). The time periodic profile covers 60° of the impeller circumference and is rotated around the diffuser inlet at the rotational speed of the impeller.

For the present simulation, time periodic inlet profiles for the inlet flow angle and the total pressure were defined. At the domain outflow plane, the mass flow was specified. Other methods of defining the inlet and outlet boundary conditions were also considered, but abandoned in favour of this technique. An alternative technique would have been to use a specified time periodic profile for the velocity at the inlet, with a static pressure condition at the outlet. The major problem with this approach is that the specified velocity profile defines the mass flow. At each time step a new inlet velocity profile would be computed by interpolation of the transient time periodic profile. The various interpolations would then result in a slightly different mass flow at the inlet for each time step and this would cause pressure oscillations throughout the domain.

The inlet total pressure profile and inlet flow angle profile were generated from data taken from the measurements. The flow angle used was that measured with the LDA system at a measurement point roughly at mid-pitch in the diffuser inlet. It was considered that this flow angle was least affected by the presence of the diffuser vanes. The total pressure condition at the inlet was determined from the measured wall static pressures (pressure transducers) and the LDA velocity measurements.

The total pressure profile at the impeller outlet and the flow angle at that radius were analyzed by Fourier transformation. This function was then used to generate smooth profiles for the inlet boundary condition (Fig. 3a). The profile covers one blade to blade section of the impeller but is extended in the pitchwise direction to allow for the pitch change between the simulations and the measurements.

The static pressure and velocity at the inlet plane of the computational domain are not constant, but result from the simulation and vary with the position of the impeller. Figure 3b shows the resulting time average of the static pressure and velocity profiles at the inlet. The influence of the diffuser vanes on the inlet flowfield is clearly visible: near partition angles of 30° and 60° there are stagnation points with high pressures and low velocities.

Computational aspects

The initial simulations were run with a simple sine profile for the radial and tangential velocities at the inlet. These simulations were used to check and debug the code with a simple time periodic inlet profile and to get a basic understanding on how the disturbances coming from the impeller pass through the diffuser. As these particular inlet boundary conditions have little in common with the real flow in the pump, the results of these simulations will not be discussed further in this paper. These simulations were used to identify a problem with the outlet boundary condition, in that reverse flow was found to occur at

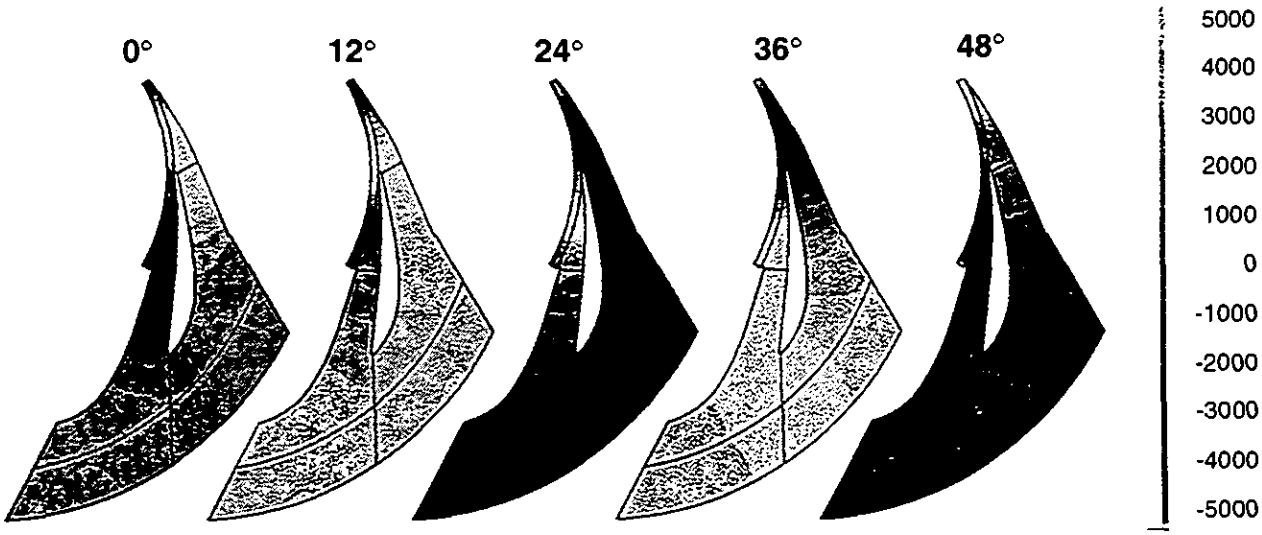

Fig. 5 Fluctuations in static pressure P (unsteady - time average, N/m^2) at impeller positions 0°, 12°, 24°, 36°, 48°

the outlet plane. The reverse flow was eliminated by the use of a constricted outlet plane in the two-dimensional simulation (the fluid was allowed to flow out of the domain in the axial direction).

To get a good initial guess for the unsteady simulations, a steady simulation was first carried out. The unsteady simulations were then restarted from these results. Best convergence was obtained by selecting a time step which is equivalent to moving the time periodic profile at the inlet in 3° steps in the circumferential direction. As a result of this 120 time steps were needed to simulate one revolution of the impeller. Converged results for each time step were obtained after having run the calculation for 240 time steps, which corresponds to 2 revolutions of the impeller.

On a IBM RS/6000 590 workstation one time step required about 5 minutes of CPU time. It was therefore possible to calculate one impeller revolution in about 10 hours. This demonstrates the enormous practical difficulty of carrying out a fully three-dimensional simulation of the entire pump impeller and diffuser, especially if no pitch change in the impeller were to be used.

Results of the two-dimensional Navier-Stokes simulations

Comparisons of steady simulation and time-average of unsteady simulations. As a first means of examining the validity of the unsteady simulation, the time-average of this simulation is compared with the steady simulation using the time-average of the inlet boundary conditions, see Figure 4. These comparisons show that there is no difference at all between the results of the two simulations in the inlet region and up to the throat of the diffuser. Downstream of the diffuser throat, small differences appear and these become magnified downstream of the diffuser vanes. The main difference between the two simulations is the extent of the wake downstream of the diffuser vane, which is substantially smaller in the steady simulation. The steady simulation also produces slightly lower pressure rise than the time-average of the unsteady simulation.

This is a very important result for the radial turbomachinery designer as it shows that at the design point there is no substantial difference between the steady simulation with time-average inlet boundary conditions and the time-average of the unsteady simulation with time varying inlet conditions. The flowfield and pressure rise predicted by these simulations is essentially identical. This is also an important result with regard to the simulation of whole turbomachinery stages. It suggests that stage calculation methods involving a mixing plane between the rotor and stator components and making use of steady calculations for the rotating and stationary domains are entirely adequate for predicting the steady performance. This may not be true for other turbomachinery configurations, for example axial turbines with strong secondary flows, see Gallus et al. (1995).

Comparisons of the unsteady flow with the time-average of unsteady flow. Important features of the unsteady aspects of the simulation are compared in figures 5, 6 and 7. These figures show the difference between the instantaneous unsteady flowfield at a particular time instant with a certain position of the impeller (0°, 12°, 24°, 36° and 48°) and the time-average of the unsteady flow field. The plots show contours of variations in static pressure, velocity levels and vorticity in the inlet region of the diffuser and in the diffuser flow channel.

The first interesting observation from these plots is the clear difference between speed of transmission of the pressure variations and the velocity variations. The changes in pressure at the inlet boundary travel practically instantaneously through the whole computation region. This can be seen best from the contours in the pressure variation figures at 12° and 24°. The shift in the impeller position between these two angles leads to a large change in the pressure level at the inlet of the domain leading into the upper diffuser channel and this pressure change is immediately felt by the whole of the upper diffuser channel. In contrast to this, the changes in the velocity and vorticity contours are convected through the diffuser at the mean flow speed.

The second observation from these plots is the different nature of the changes in the amplitude of the variations of the pressure and velocity fluctuations as they are transmitted through the diffuser. The velocity and vorticity fluctuations are very strong at the inlet to the diffuser and become weaker as they are convected downstream. Shortly

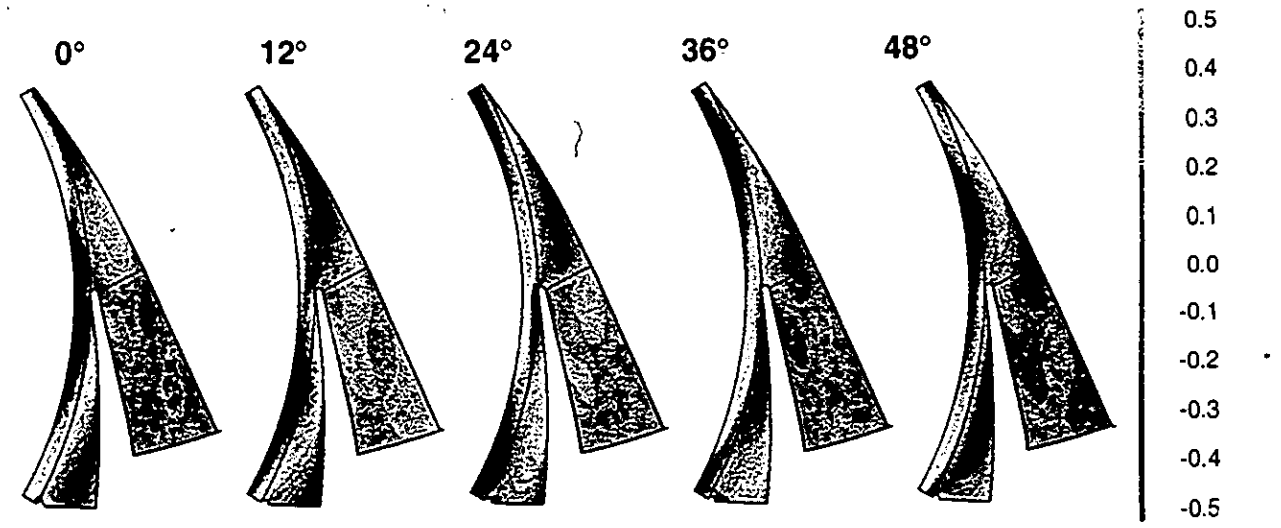

Fig. 6 Fluctuations in velocity level w (unsteady - time average, m/s) at impeller positions 0°, 12°, 24°, 36°, 48°

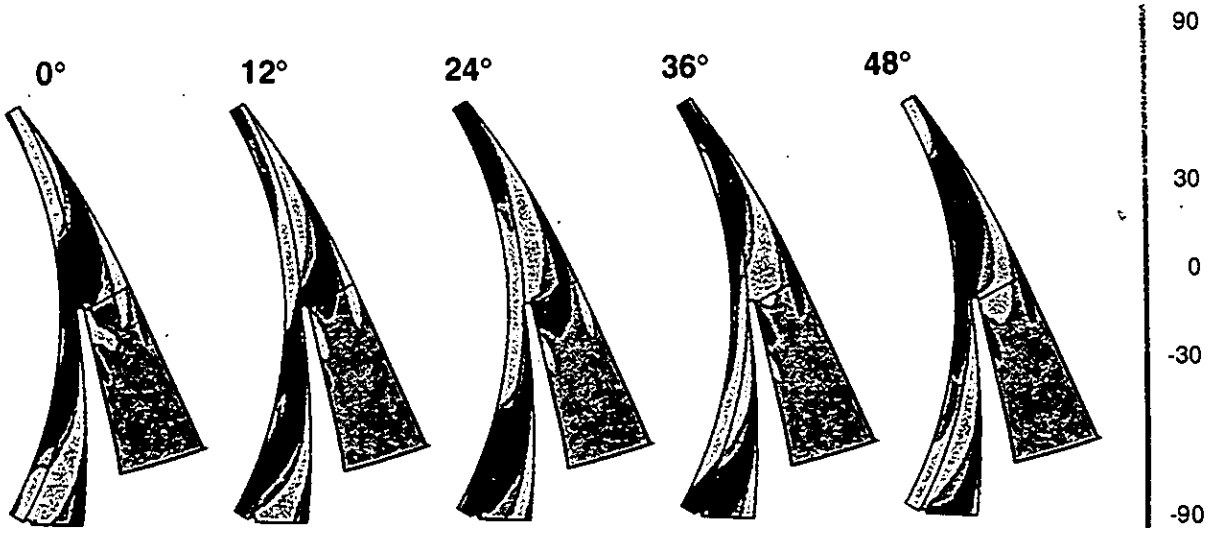

Fig. 7 Fluctuations in vorticity (unsteady - time average, 1/s) at impeller positions 0°, 12°, 24°, 36°, 48°

downstream of the throat the cyclical fluctuations in velocity have less than 20% of their magnitude at the inlet to the domain. The pressure fluctuations decay less strongly as they pass through the diffuser.

The structure of the unsteady velocity field in the diffuser is shown in the vector plots in figure 8a, for several positions of the impeller (0°, 12°, 24°, 36° and 48°). These vectors show the periodic component of the velocity only, i.e. the time average of the local velocity has been subtracted from the calculated value. A vector pointing in the reverse flow direction does not indicate reverse flow but simply identifies that at this time instant the current velocity level is less than the average value at this point. It can be seen that the jet wake nature of the flow at the diffuser inlet develops into a pair of vortices of opposing sign which are convected into the diffuser and decay as they move downstream. The vector plots at different positions of the impeller show that the flow field is strongly unsteady up to the throat of the diffuser (long vectors with large changes in position), whereas downstream of the throat there are only very small differences between the vectors at different impeller positions. A velocity peak occurring at the inlet decays very rapidly and has only a little impact on the unsteady flowfield downstream of the diffuser throat.

Comparison of simulations with measurements. Before describing the comparisons between the simulations and the test data it should be pointed out that the simulations are based on a two-dimensional grid without endwalls and the measurements are, of course, fully three dimensional so that some of the differences in the comparisons may be due to three-dimensional effects. In order to reduce these differences to a minimum, the comparisons given below are mainly based on measurements in the mid-span plane of the diffuser.

Figure 9 compares the measured and calculated velocity vectors for four different positions of the impeller blade. Up to the throat of

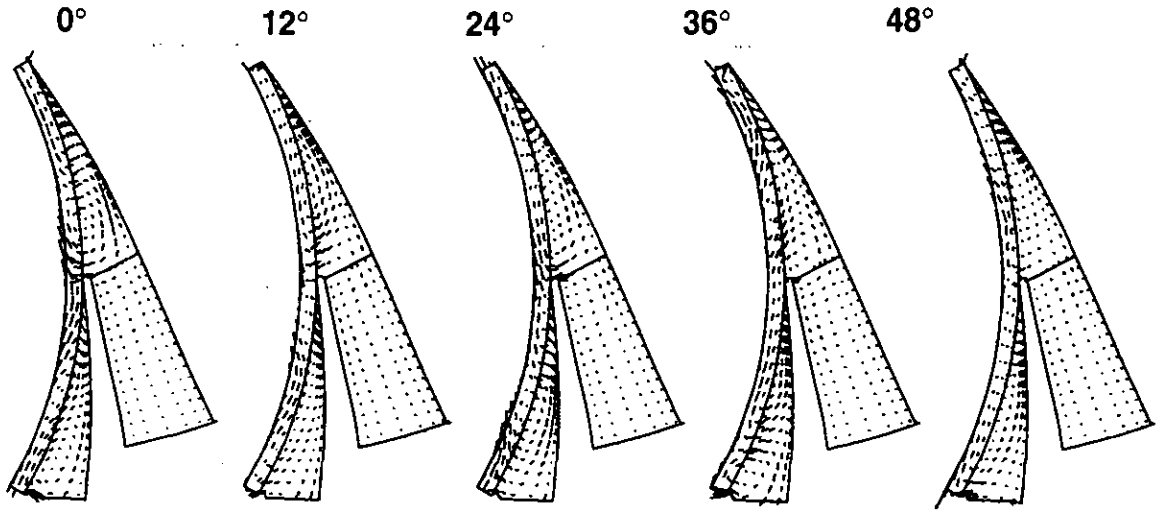

Fig. 8A Fluctuations in velocity vectors (unsteady - time average) at impeller positions 0°, 12°, 24°, 36°, 48°

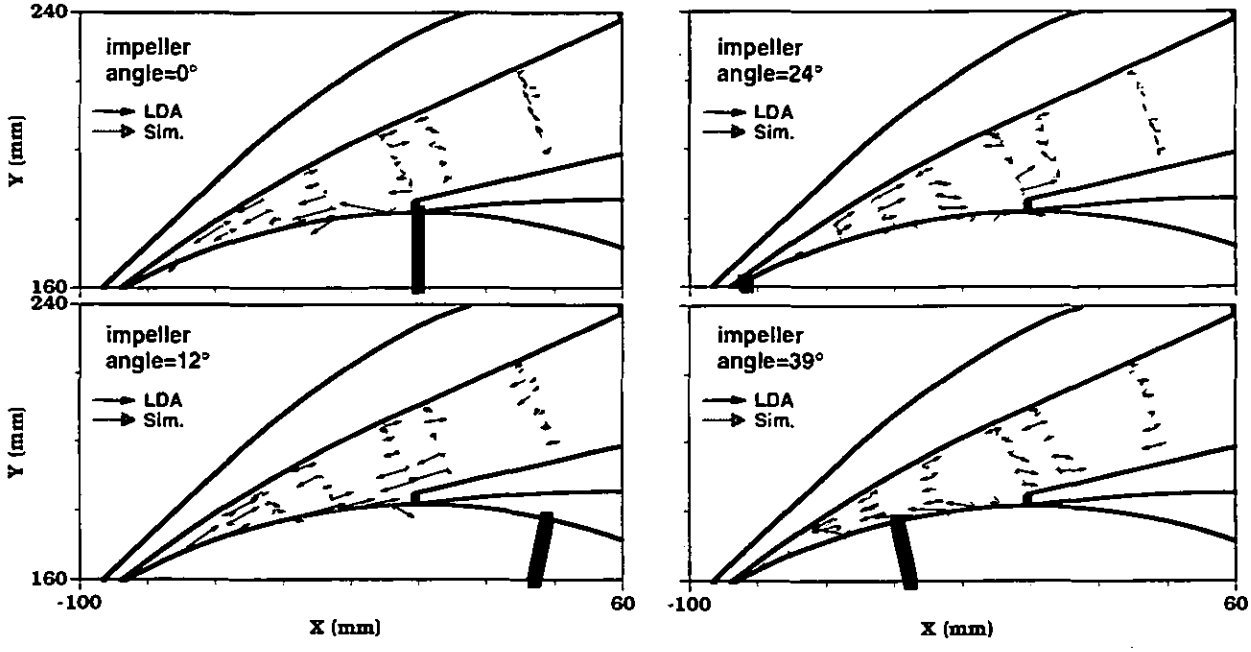

Fig. 8B Measured and calculated fluctuations in velocity vectors (unsteady - time average) at 4 impeller positions

the diffuser the agreement is quite good, especially in terms of the flow direction, such that the simulation predicts the angle of attack of the flow onto the diffuser vane quite well. After the throat the simulation starts to diverge from the measurements. This is due to the three-dimensional nature of the flow, see Casey et al. (1995a, b), where it is shown that a flow separation at the throat of the diffuser on the hub-side of the flow channel was present in the test rig.

The unsteady measured and calculated flow fields in the diffuser for four different positions of the impeller blade are shown in figure 8b. Like in figure 8a these vectors show only the unsteady periodic component of the velocity. The calculated vectors at the inlet of the diffuser are significantly shorter than the measured ones. This indicates that the unsteadiness of the flow field near the inlet is under predicted by the simulations. Figure 10 shows too, that the measured velocity amplitudes are higher than the calculated ones, especially at the inlet.

The time periodic velocity components in the mid-span plane of the diffuser were measured by LDA. Figure 10 shows a comparison of the velocity level from these measurements at six points along the centerline of the diffuser for a variation of the impeller rotational position. The agreement is not that good, although the simulations and

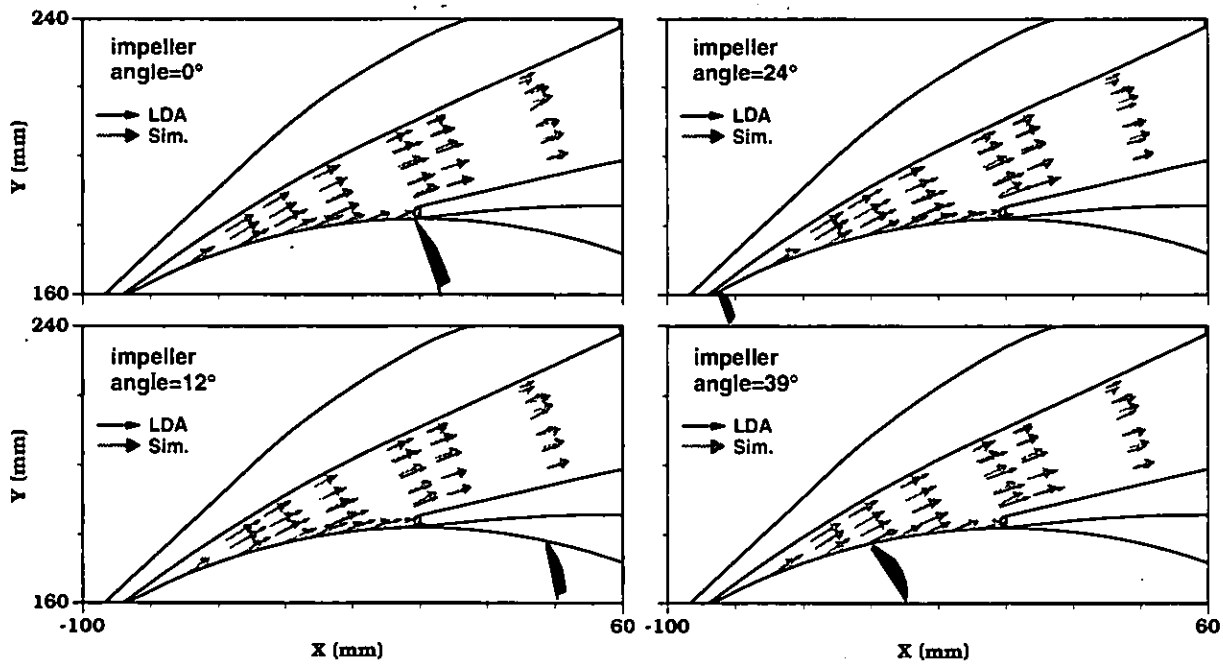

Fig. 9 Measured and calculated velocity vectors at 4 impeller positions

experiments show that the velocity level and the amplitude of the velocity fluctuations both decrease along the diffuser. In most points the level and amplitude of the measured velocities are higher than the calculated ones.

Unsteady pressure measurements were carried out in the test rig on the hub and shroud side of the diffuser at three points along the centerline (points 1, 2, 4 in figure 11). The comparison of the measured and calculated static pressure along the middle of the diffuser channel shows slightly better agreement than for the velocities, see figure 11. The comparison shows that the phase variations of the pressure fluctuations

$$\Delta p^* = \frac{\Delta p}{\frac{\rho}{2} u_2^2}[-] \qquad (1)$$

is well captured, but that the amplitudes are over predicted at point 1 near the inlet, but agree quite well with the measurements further downstream (points 2 and 4). The blade passing frequency is clearly visible in the calculated pressure field at all points along the diffuser, decreasing in amplitude towards the exit.

A further comparison between the test data and the simulations is given in figure 12. This shows the measured fluctuations in vorticity in the diffuser flow channel as a function of the impeller blade position, and can be compared to the simulations of this given in figure 7. This data has been obtained from the PTV velocity measurements in the mid-plane of the diffuser. In the test pump the wake of the impeller blade produces regions with high positive and high negative vorticities, whereby the strength of the positive and negative vorticity regions is the same. The vorticities are convected through the diffuser at the mean flow velocity and disappear rapidly downstream of the throat of the diffuser, showing essentially similar flow structures to those simulated.

FURTHER WORK

Work on this project is continuing and is directed towards more complex simulations of the flow. An unsteady 3D simulation of the diffuser flow with a time periodic inlet profile from an impeller simulation is currently being carried out and a fully 3D simulation of the impeller and diffuser flow is planned. In addition work is continuing on the examination of the measurements at other operating points, examination of the flow in the same diffuser with a different impeller and examination of diffuser flows in other pump configurations.

CONCLUSIONS

The calculations presented here are the first simulations of the unsteady flow in a vaned pump diffuser using a commercially available general purpose Navier Stokes CFD code. The measurements and simulations have identified some of the interesting flow structures and effects that occur at the best efficiency point in the diffuser due to the passage of wakes and potential disturbances from the impeller. The important conclusions from this work are as follows:

- There is no substantial difference between the steady simulation and the time-average of the unsteady simulation in terms of the flowfield and pressure rise predicted by these simulations. This is a useful result for the radial turbomachinery designer as it implies that at the design point steady simulations of diffuser flows as currently used in routine design calculations are not largely in error. It also implies that the unsteady effects are well predicted by a linear analysis (Saxer et al., 1994).

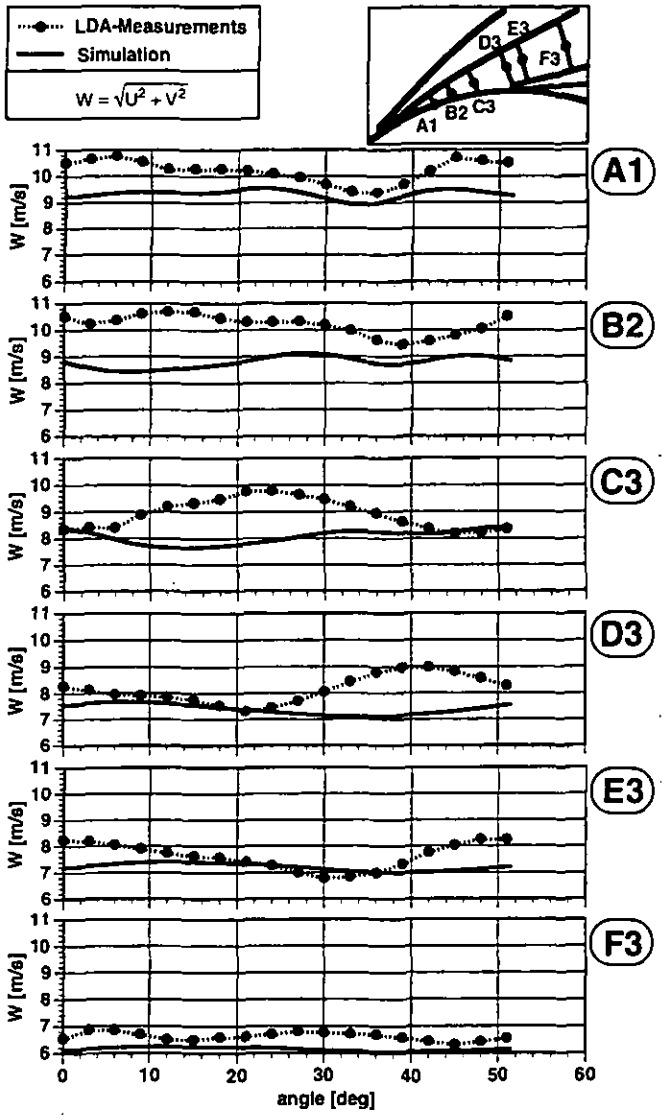

Fig. 10 Measured and calculated velocity level w along the diffuser center line

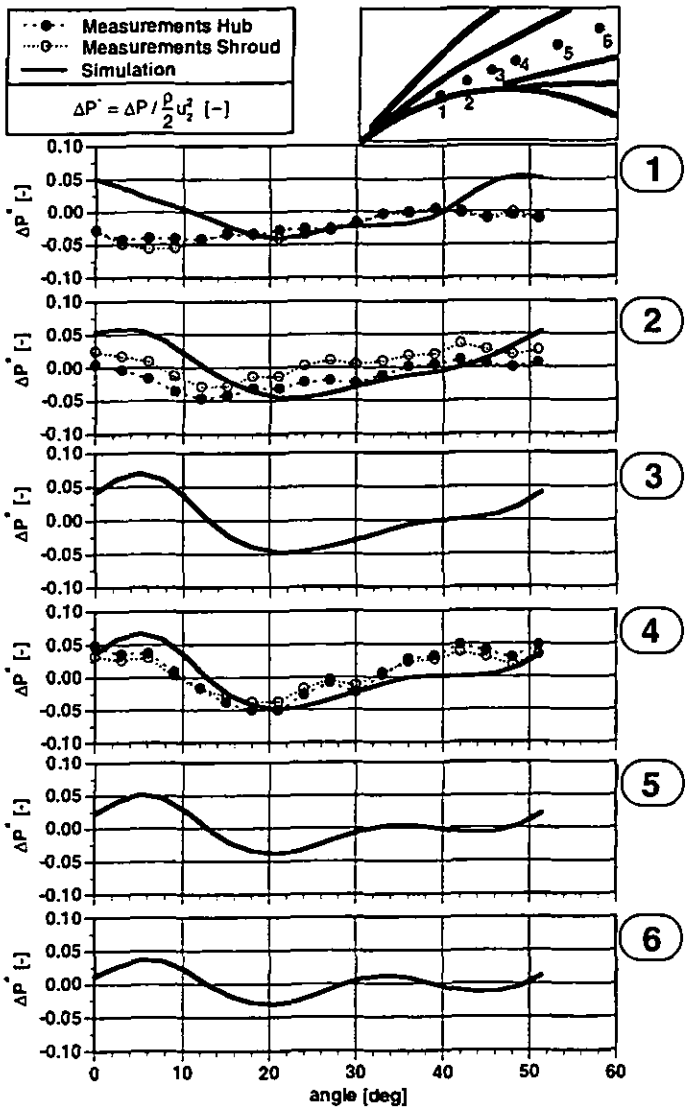

Fig. 11 Measured and calculated pressure along the diffuser center line

• The relatively simple two-dimensional simulation using a time-periodic inlet profile to represent the impeller explains clearly how the periodic disturbances from the impeller pass through the diffuser. Velocity disturbances are convected downstream into the diffuser at the mean flow speed, whereas pressure disturbances are felt more or less instantaneously at the same time at any point in the diffuser.

• The results of the unsteady simulation are in good qualitative agreement with the unsteady measurements from the test rig, and both show the passage and decay of the impeller blade wakes through the diffuser. The test data and the simulations show that the magnitude of the periodic unsteadiness in the diffuser is strongest at impeller outlet and diminishes rapidly downstream of the diffuser throat.

• The two-dimensional simulation with a time periodic profile to represent the wakes and potential interaction effects from the impeller shows that many of the important phenomena involved in the impeller/diffuser interaction can be examined on this basis without the need for a full unsteady rotor/stator simulation.

REFERENCE

ASC, 1994, TASCflow Documentation Version 2.3, Advanced Scientific Computing Ltd., Waterloo, Ontario, Canada.

Casey, M. V., 1994, "The industrial use of CFD in the design of Turbomachinery", AGARD Lecture Series *Turbomachinery design using CFD*, AGARD LS-195.

Casey, M. V., Eisele, K., Zhang, Z., Gülich, J., and Schachenmann, A., 1995a, "Flow Analysis in a pump diffuser, part 1: LDA and PTV flow measurements of the unsteady flow", ASME paper 1995 FED Summer Meeting, *Symposium on Laser Anemometry.*

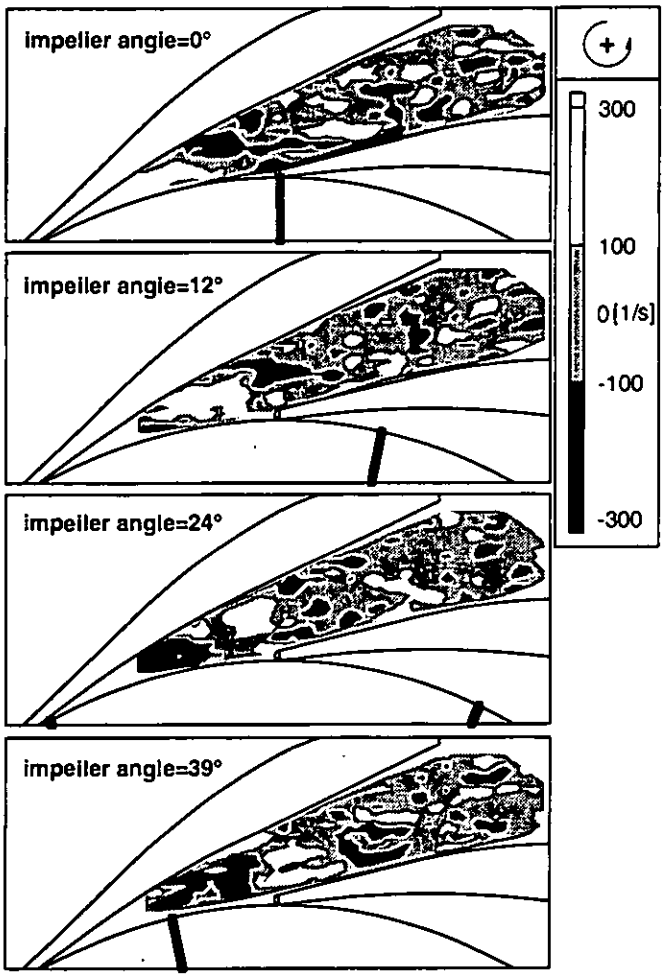

Fig. 12 Measured fluctuation in vorticity at 4 impeller positions

Casey, M. V., Eisele, K., Muggli, F. A., Gülich, J., and Schachenmann, A., 1995b, "Flow Analysis in a pump diffuser, part 2: Validation of a CFD Code for Steady Flow", ASME paper 1995 FED Summer Meeting, *Symposium on Numerical Simulations in Turbomachinery*.

Chu, S., Dong, R. and Katz, J., 1995, "Relationship Between Unsteady Flow, Pressure Fluctuations and Noise in a Centrifugal Pump – Part A: Use of PDV Data to Compute the Pressure Field", Journal of Fluids Engineering, Vol. 117, pp. 24-29.

Dalbert, P. and Wiss, D., 1995, "Numerical transonic flow field predictions for NASA compressor rotor 37", ASME Gas Turbine Conference, Houston.

Dawes, W. D., 1994, "A simulation of the unsteady interaction of a centrifugal impeller with its vaned diffuser: flows analysis" ASME Paper 94-GT-105.

Eisele, K., Muggli, F. and, Schachenmann, A., 1992, "Investigation of Flow Phenomena in Multistage Pumps", 6th International Symposium on Applications of Laser Techniques to Fluid Dynamics, Lisbon, Portugal.

Eisele, K., Muggli, F. et al., 1993, "Pump Development with Laser and Computer", *Technical Review Sulzer*, 93/2, pp. 37-39.

Eisele, K., Zhang, Z., Hirt, F. and Perschke, N., 1995,"A new simple and robust Particle Image Velocimetry Technique for Industrial Research", to be published.

Eisele, K., Zhang, Z. and Muggli, F., 1994, "Investigation of the Unsteady Diffuser Flow in a Radial Pump", 7th International Symposium on Applications of Laser Techniques to Fluid Dynamics, Lisbon, Portugal.

Gallus, H. E., Zeschky, J. and Hah, C., 1995, "Endwall and Unsteady Flow Phenomena in an Axial Turbine Stage", Journal of Turbomachinery, Vol. 117, pp. 562-570.

Giles, M. and Haimes, R., 1993, "Validation of a Numerical Method for Unsteady Flow Calculations", Trans. ASME Journal of Turbomachinery, Vol. 115, pp. 110-117.

Grant, I. and Liu, A., 1990, "Directional ambiguity resolution in particle image velocimetry by pulse tagging", Experimens in Fluids, Vol. 10, pp. 71-76, reprinted in Selected Papers on PTV, SPIE Milestone Volume MS 99 Editor Ian Grant 1994.

Gülich, J., Bolleter, U., 1992, "Pressure Pulsations in Centrifugal Pumps", Journal of Vibration and Acoustics, Vol. 114, pp. 272-279.

Gülich, J., Egger, R., 1992, "Part-Load Flow and Hydraulic Stability of Centrifugal Pumps", Empire State Electric Energy Research Corporation and Electric Power Research Institute, final report.

Korakianitis, T., 1993, "On the Propagation of Viscous Wakes and Potential Flow in Axial-Turbine Cascades", 36th International Gas Turbine and Aeroengine Congress and Exposition, Orlando, Florida.

Renau, L. R., Johnston, J. P. and Kline, S. J.,1967, "Performance and Design of Straight, Two-Dimensional Diffusers", *ASME Journal of Basic Engineering*, pp. 141-150.

Saxer, A. P. and Giles, M. B., 1994, "Predictions of Three-Dimensional Steady and Unsteady Inviscid Transonic Stator / Rotor Interaction with the Inlet Radial Temperature Nonuniformity", Journal of Turbomachinery, Vol. 116, pp. 347-357.

Schachenmann, A., Muggli, F., and Gülich, J., 1993, "Comparison of three Navier-Stokes Codes with LDA-Measurements on an Industrial Radial Pump Impeller", ASME Fluids Engineering Conference, Washington D.C.

Zhang, Z. and Eisele, K., 1995, "Off-axis alignment of an LDA-probe and the effect of astigmatism on measurements" to be published in Experiments in Fluids.